NASA TECHNICAL MEMORANDUM

NASA TM X-52827

NASA TM X-52827

FLIGHT AND WIND TUNNEL INVESTIGATION OF INSTALLATION EFFECTS ON UNDERWING SUPERSONIC CRUISE EXHAUST NOZZLES AT TRANSONIC SPEEDS

by Daniel C. Mikkelson and Bernard J. Blaha
Lewis Research Center
Cleveland, Ohio

TECHNICAL PAPER proposed for presentation at
AGARD 1970 Aerodynamic Interference Specialists
Meeting sponsored by AGARD Fluid Dynamics Panel
Silver Spring, Maryland, September 28-30, 1970

FLIGHT AND WIND TUNNEL INVESTIGATION OF INSTALLATION EFFECTS ON UNDERWING SUPERSONIC CRUISE EXHAUST NOZZLES AT TRANSONIC SPEEDS

by Daniel C. Mikkelson and Bernard J. Blaha

Lewis Research Center
Cleveland, Ohio

TECHNICAL PAPER proposed for presentation at
AGARD 1970 Aerodynamic Interference Specialists Meeting
sponsored by AGARD Fluid Dynamics Panel
Silver Spring, Maryland, September 28-30, 1970

NATIONAL AERONAUTICS AND SPACE ADMINISTRATION

SUMMARY

To investigate airframe installation effects on exhaust nozzle systems mounted on underwing engine nacelles, a combined flight and wind tunnel test program is being conducted utilizing a modified F-106 aircraft. Flight tests were conducted in the transonic speed regime to determine nozzle performance and boattail drag for variable flap ejector, conical plug, and auxiliary inlet ejector nozzle concepts. Wind tunnel tests were conducted on isolated models of these nozzles and also on a 1/20-scale model of the F-106 aircraft with simulated underwing engine nacelles. Wing and nacelle pressures from these wind tunnel tests are used to qualitatively explain the observed installation effects. The 1/20-scale model was also used to evaluate the effects of changes in nacelle geometry and angle-of-attack.

FLIGHT AND WIND TUNNEL INVESTIGATION OF INSTALLATION EFFECTS ON UNDERWING SUPERSONIC CRUISE EXHAUST NOZZLES AT TRANSONIC SPEEDS

By Daniel C. Mikkelson and Bernard J. Blaha
Lewis Research Center
National Aeronautics and Space Administration
Cleveland, Ohio

E-5725

INTRODUCTION

As part of a broad program in airbreathing propulsion, the NASA-Lewis Research Center is investigating the effects of the airframe flow field on the performance of exhaust nozzle systems appropriate for use at supersonic speeds. Experience has shown that performance of an exhaust nozzle system can be appreciably affected by installation on an aircraft, especially at off-design conditions [1]. One of the more desirable locations for the propulsion system of airplanes which must operate efficiently at both subsonic and supersonic speeds is in aft-mounted underwing nacelles. With this location the nacelle inlet is shielded by the wing lower surface to minimize angle-of-attack effects. Also, other favorable interference effects between the wing and nacelle flow fields may minimize drag at important flight conditions. This location has not been used in previous supersonic aircraft, and the effects of such an installation on the exhaust systems required for this type of aircraft are not well understood. Wind tunnel tests are used extensively to evaluate these installation effects. However, accurate data is particularly hard to obtain in wind tunnel facilities at transonic speeds because models are limited to very small sizes to avoid wall interference effects.

To investigate installation effects on the exhaust system of a podded engine installation of this type, a combined flight and wind tunnel test program is being conducted utilizing a modified F-106 aircraft with underwing engine nacelles housing J85-GE-13 afterburning turbojet engines. The F-106 aircraft was selected for this program because it has a wing planform which could be representative of present and future high performance supersonic aircraft. The aircraft provides the capability of investigating complete propulsion systems using larger and more complex hardware with more complete instrumentation than is possible with wind tunnel models. Some of the early flight results are presented in Refs. [2 and 3].

In a concurrent effort, wind tunnel models are also being used to investigate configuration changes that would be too expensive, time consuming, and in some cases impossible to test on the F-106 aircraft. Such a series of tests was conducted in the Lewis 8- by 6-Foot Supersonic Wind Tunnel using a 1/20-scale model of the F-106 aircraft with simulated underwing engine nacelles. Some of the early wind tunnel test results are presented in Refs. [4-6]. Although small in size, this model has been very useful in qualitatively explaining the installation effects observed both in flight and in wind tunnel tests. Because of the small size of the test nacelles on this model, only simple variable flap ejector nozzles could be studied and jet effects were simulated with solid surfaces. In addition to the 1/20-scale F-106 model, and 8-1/2 inch (21.59 cm) diameter cold-jet model was used to obtain isolated boattail drag and nozzle performance [7 and 8]. Also a nacelle was tested under a simulated wing [9]. The simulated wing test included a cylindrical nacelle installed close to the lower surface of a rectangular flat plate wing simulator. This test was an early attempt to investigate installation effects on larger-sized nacelles in the 8- by 6-foot Supersonic Wind Tunnel with only portions of the wing and airframe present. In this paper, boattail pressure drag coefficients for the isolated and installed wind tunnel models are presented and compared with flight test results. Comparisons of flight and wind tunnel nozzle gross thrust coefficients are presented for several competitive exhaust nozzle types. In addition, 1/20-scale model nacelle and wing pressure distributions are presented to qualitatively explain the observed installation effects.

AIRCRAFT AND MODEL DETAILS

The modified F-106 aircraft is shown in Fig. 1 with a plug nozzle mounted on one of the underwing engine nacelles. The nacelles were located at approximately 32 percent semispan and had a cylindrical diameter of 25.0 inches (63.50 cm). The engine nacelle installation mounted under the wing is shown schematically in Fig. 2. The nacelles were strut mounted at a -4.5° incidence angle relative to the wing chord with the exhaust nozzles overhanging the wing-trailing edge. Because of this overhand, the elevon section immediately above the nacelles was cut out and rigidly fixed to the wing. The nacelles incorporated normal shock inlets that faired into a bulged section on the bottom of the nacelle. This faired bulged section was needed to accommodate the J-85 engine accessory package. The effect of this bulged section on nozzle boattail drag was shown to be small for a variable flap ejector nozzle [4].

The nacelles were supported by two attachment links that were normal to the nacelle axis, and all axial forces were transmitted through a load cell to the wing. This load cell measured the nacelle net thrust-minus-drag and was compensated for any axial acceleration and gravity component [3]. Nacelle drag forward of the exhaust nozzle was determined during prior calibration flights with a simple reference nozzle. Calibrated J-85 engines and secondary flow valves were used to determine the flow conditions entering the nozzles. The research nozzle gross thrust-minus-drag was determined by subtracting the nacelle drag (forward of the nozzle) from the load-cell reading. An onboard digital data system was used to record aircraft and nacelle parameters. Flight tests were conducted over the Mach number range from 0.5 to 1.3 at corresponding angles-of-attack from 8° to 1° and Reynolds numbers from 2.3×10^{6} per foot (0.8×10^{5} per cm) to 4.4×10^{6} per foot (1.4×10^{5} per cm), respectively.

A photograph of the 1/20-scale model of the F-106 aircraft is shown in Fig. 3 with nacelles that were scaled versions of those tested in flight. Open inlets which allowed air to flow through the nacelles and jet-boundary simu-

lators are shown. However, both flow-through and closed nacelles with and without the bulged section were tested. In addition, several other nacelle shapes were investigated. Wind tunnel tests were conducted over a range of Mach numbers from 0.56 to 1.46 at angles-of-attack from 0^{o} to 15^{o}. Reynolds number varied from 3.60×10^{6} per foot (1.18×10^{5} per cm) at Mach number 0.56 to 4.96×10^{6} per foot (1.63×10^{5} per cm) at Mach number 1.46. All of the nacelles were tested with 15^{o} conical boattails with zero (sharp corner) radius of curvature at its juncture with the nacelle. The boattail-trailing edge extended 0.975 nacelle diameters aft of the wing-trailing edge.

The exhaust nozzles tested are shown in Fig. 4. With the variable flap ejector (VFE) nozzle type, the variation in internal expansion ratio which is required for efficient operation over a wide nozzle pressure ratio range is obtained by modulating the position of the variable shroud flaps. The VFE nozzle which was tested had a 15^{o} boattail that simulated the position of the nozzle variable flaps when the exit area is reduced for operation at subsonic and transonic speeds.

The 10^{o} half-angle conical-plug nozzle is of interest because the sliding shroud is a relatively simple mechanism for varying the internal expansion ratio. Also plug nozzles provide an opportunity for infrared suppression in military applications and may be quieter than other nozzle types [10]. This nozzle, however, does require added complexity for cooling the plug, especially during reheat operation. The conical trailing end of the plug can be truncated as shown by the dotted lines and some airflow into the base region will minimize its drag.

The auxiliary inlet ejector (AIE) nozzle used 16 small inlets to take tertiary air from over the wing and around the nacelle and exhaust it with the primary and secondary streams. This additional air helps fill up the divergent shroud to minimize overexpansion losses at low nozzle pressure ratios. Therefore, the trailing flaps do not have to close as far, thus reducing boattail projected area. Also nozzle weight may be reduced if free-floating inlet doors and trailing flaps can be used rather than the more complex mechanically-actuated designs. This nozzle was installed with a wing cutout which provided flow from above the wing to the top three auxiliary inlets.

RESULTS

Installation Effect on Nozzle Performance

A comparison of flight and wind tunnel boattail drag data for a VFE nozzle with a 15^{o} sharp-corner boattail (zero radius of curvature) is shown in Fig. 5 at a nominal angle-of-attack of 2.5 degrees. Flight data are presented and compared with installed wind tunnel data from the 1/20-scale F-106 model [6], and data from a 4-inch (10.16 cm) diameter model under a rectangular flat-plate-simulated wing [9]. Comparisons are also made with isolated data from an 8-1/2 inch (21.59 cm) diameter cold-jet model [7]. The flight data presented were obtained with the J-85 engine at maximum afterburning, which provided a nozzle pressure ratio and area ratio such that the cylindrical ejector nozzle was overexpanded below Mach 1.0 and flow full above Mach 1.0. Similar conditions existed for the cold-jet nozzle. Jet-boundary simulators were used on the 1/20-scale F-106 model and on the model with the simulated wing. Their constant cylindrical cross section simulated a nozzle operating fully expanded over the entire speed range. It is apparent that installation of this nozzle on the airframe caused a significant decrease in boattail drag compared to the isolated nozzle. This drag reduction was very large at high subsonic speeds and the transonic drag rise was delayed to Mach 0.97. The flight and wind tunnel installed drag data compared favorably except near Mach 1.0 where the flight values were considerably higher. It is also apparent that some of this drag reduction was obtained with just a flat-plate wing simulation. The further decrease in nozzle afterbody drag seen at Mach 0.95 for the installed flight and 1/20-scale model data, as will be shown in later figures, was the result of the nacelle and wing transonic terminal shocks being located near the boattails at these speeds. Terminal shocks were also present on the cold-jet model and the model with the simulated wing, but due to tunnel blockage the effect on afterbody drag was delayed to Mach 1.08 and 1.02, respectively.

The effect of nozzle afterbody shape on boattail drag is shown in Fig. 6 for a VFE nozzle with a 15^{o} boattail angle. Installed flight and 8-1/2 inch (21.59 cm) diameter isolated cold-jet data are presented for values of boattail juncture radius to nozzle diameter ratios (radius ratio) of 0 and 2.5. With the isolated nozzle, a significant subsonic drag reduction was obtained when the radius ratio was increased from 0 to 2.5. The installation effect, however, produced a larger reduction in subsonic drag for the radius ratio 0 (sharp corner) boattail. For the rounded-corner boattail (with a radius ratio of 2.5) the installation effect was considerably less and resulted in installed boattail drags that were only slightly lower than the sharp-corner boattail. The drag reduction due to radius ratio was generally unaffected by the installation in the supersonic region.

The effect of installation on nozzle gross thrust coefficient is shown in Fig. 7 for the VFE, conical plug, and AIE nozzles. Flight data were obtained with the J-85 engine at minimum afterburning for all nozzles except the conical plug which was tested at military power because of plug-cooling limitations. At these power settings the nozzle nominal pressure ratio schedule ranged from 3.2 at Mach 0.7 to 5.6 at Mach 1.3. Isolated data were obtained with the 8-1/2 inch (21.59 cm) diameter cold-jet model at similar operating conditions. All data were obtained at a nominal corrected secondary-to-primary weight-flow ratio of 0.04.

For the VFE nozzle with a 15^{o} sharp-corner boattail (radius ratio of zero), the installed boattail drag trends shown in Figs. 5 and 6 resulted in the improved installed nozzle gross thrust coefficient (as compared to isolated data) across the entire speed range as shown in Fig. 7(a). The nozzle gross thrust coefficient is defined as the measured nozzle gross thrust-minus-drag ratioed to the ideal thrust of the engine primary. At Mach 0.9 the 3-percent improvement in installed nozzle coefficient would be equivalent to an approximate 6-percent reduction in total aircraft drag for a large supersonic cruise aircraft operating off-design at part power. The isolated nozzle data between Mach 1.0 and 1.2 was influenced somewhat by wind tunnel wall-interference effects on terminal shock movement over

the nozzle. The significant improvement in nozzle performance with the sharp-corner boattail generally correlated with the decrease in boattail drag seen previously. However, with the rounded-corner boattail (radius ratio 2.5) the change in performance would generally be small because the installation effect on boattail drag was significantly less.

For the conical plug nozzle with a 17° boattail angle and retracted shroud (fig. 7(b)), a large favorable installation effect occurred between Mach 0.89 and 0.97. Above Mach 0.97 the installed nozzle coefficient was significantly lower than the isolated data; however, below Mach 0.89 the installed data was only slightly lower than isolated results. This nozzle was probably more sensitive than the others to external flow because it was operated at military power instead of minimum afterburning.

For the AIE nozzle with a 15° boattail angle and radius ratio of 0.5 (fig. 7(c)), the isolated and installed nozzle results compared favorably at all Mach numbers tested. Below Mach 0.86 the installed data was slightly lower than the isolated results. However, this trend was reversed between Mach 0.86 and 0.98. Even though the installation effect caused a large reduction in the boattail drag of this nozzle just as it did for the VFE nozzle, this benefit was apparently offset by reduced performance of the auxiliary inlets. These inlets did not perform as well as they did in isolated nozzle tests because the installation effects created thick and unsymmetrical boundary layers ahead of the inlets [2] which were not duplicated when tested as isolated components.

It is apparent that the effect of airframe installation on nozzle performance for an installation of this type is strongly dependent on the nozzle design concept. Favorable and unfavorable effects are obtained, and in some cases these effects are compensating so that the overall effect is minor. However, the VFE nozzle with a sharp corner (zero radius ratio) seemed to benefit most from the installation effects since its performance was improved across the entire speed range.

Flow Field in Region of Exhaust Nozzle

Wing and nacelle pressure distribution data obtained with the 1/20-scale F-106 model will be used, in the next few figures, to qualitatively explain the observed installation effects. Model data are used because the wing on this model was more extensively instrumented than the wing on the aircraft. Also installed F-106 data with "clean" nacelles (no bulge) was available only from this model. However, similar pressure distribution trends were obtained in flight.

The installation effects on nozzle boattail drag and performance was the results of the effects of the combined wing and nacelle flow fields and are apparent in the wing and nacelle pressure distributions. The average wing lower surface pressure distribution without nacelles is shown in Fig. 8. Data are presented for Mach numbers from 0.8 to 1.0 at 2.5° angle-of-attack. These wing pressures are averages of those obtained between 20 and 43 percent semispan. The wing cross section at the (32 percent) nacelle semispan location is shown for reference. It is apparent that a region of low pressure existed on the wing lower surface aft of the wing maximum thickness point (which was approximately 50-percent chord) and was followed by a recompression near the wing-trailing edge. An increase in Mach number resulted in lower pressures in this region and a much stronger recompression further aft. Near Mach 0.95 this recompression had the characteristics of a terminal shock. At Mach 1.0 this shock moved off the wing and the pressure remained low to the wing-trailing edge. This shock movement correlated with the installed boattail drag rise and drop in nozzle performance seen near Mach 0.97 in Figs. 6 and 7, respectively.

The effect of the nacelle installation on the wing lower surface pressure distribution is shown in Fig. 9 for Mach 0.85 at 2.5° angle-of-attack. Pressures are shown for one row of orifices just outboard of the nacelle location; however, the observed effects extended over considerable regions of the wing lower surface. With the nacelles installed, a region of increased pressure occurred above the forward half of the inlet cowl. The pressures above the center portion of the nacelle was lower than without the nacelles and were followed by a stronger recompression near the wing-trailing edge. The lower pressures above the center portion of the nacelle probably resulted from the expansion region generated by the flow turning at the cowl nacelle juncture. These modifications to the wing pressure distribution, as described in Ref. 2, resulted in elevon trim changes for the aircraft especially at transonic speeds.

The installation effect on the nacelle pressure distribution is shown in Fig. 10 for a cylindrical nacelle (no bulged section) at Mach 0.95 and 0° angle-of-attack. The isolated nacelle pressures showed a typical flow overexpansion at the cowl-nacelle juncture and recompression for this Mach number. With the nacelle installed, the flow overexpansion extended to further aft positions on the nacelle. These lower nacelle pressures were apparently due to the combination of the following wing and nacelle flow field characteristics: 1) the low pressures that occurred in this region on the isolated wing at high subsonic speeds; 2) the flow expansion at the cone-cylinder juncture on the nacelle; and 3) the reflection of this expansion from the wing lower surface. The flow recompression, being further aft on the nacelle, coincided with the strong recompression region seen on the isolated wing in Figs. 8 and 9. Therefore, at the high subsonic speeds the nozzle was immersed in the combined recompression fields of both the nacelle and wing. These changes in the nozzle flow field compared to the isolated nozzle case resulted in higher boattail pressures and thus lower drag. This result is particularly evident for the sharp-corner boattail (radius ratio, 0) and to a considerably lesser degree for the rounded-corner boattail (radius ratio 2.5) seen previously in Fig. 6. As seen in Fig. 11 at Mach numbers 0.90 and 0.95, the low pressures forward on the nacelle recompressed through a pressure discontinuity region, or terminal shock, which moved aft with increasing Mach number. At Mach 0.95, this pressure discontinuity coincided with the location of the terminal shock seen at the wing-trailing edge without nacelles in Fig. 8. At Mach 1.00, the pressure discontinuity region moved aft of the nacelle and the decreased pressures on the boattail resulted in the sharp drag rise observed previously at Mach 0.97.

The effect of angle-of-attack on installed boattail drag is shown in Fig. 12 for angles-of-attack from 2.5° to 15°.

Over the Mach number range investigated, the effect of increasing angle-of-attack was small for angles less than 8.5°. Near Mach 1.0 increasing angle-of-attack resulted in reduced boattail drag.

Large variations in nacelle shape were also found to generally have little effect on boattail drag as shown in Fig. 13. Data were obtained at 2.5° angle-of-attack for cylindrical, bulged (as on the F-106), flared, and flared-bent nacelle shapes. These nacelle shapes are illustrated with schematic drawings in Fig. 13. Flow-through nacelles that allowed the stream flow to pass through the nacelle body were used. The effect of nacelle shape was small except for the flared nacelle where the boattail drag was considerably increased with values similar to isolated nacelle results. This was probably the result of significant differences in the flow field around the forward portions of this nacelle in contrast to that of the others. The flared nacelle differed from the other designs by eliminating the flow spillage at the cowl lip and the cone-cylinder juncture below the wing surface. As shown in Ref. 6, the installation effects with the nacelle further outboard on the wing were similar to those observed at the inboard station.

CONCLUSIONS

To investigate airframe installation effects on exhaust nozzle systems mounted on underwing engine nacelles, a combined flight and wind tunnel test program was conducted utilizing a modified F-106 aircraft. Flight tests were conducted on variable flap ejector (VFE), conical plug, and auxiliary inlet ejector (AIE) type nozzles. Wind tunnel tests were conducted on isolated models of these nozzles and also on a 1/20-scale model of the F-106 aircraft with simulated under-wing engine nacelles. Results from these wind tunnel tests were used to qualitatively explain the observed installation effects. Conclusions which can be made are:

1. An airframe installation of this type resulted in reduced drag at all Mach numbers except near Mach 1.0 for the sharp-corner boattail of a variable flap ejector (VFE) nozzle. In addition, transonic boattail drag rise was delayed to Mach 0.97. At subsonic speeds, installing a rounded-corner boattail (radius ratio 2.5) only slightly reduced its drag. This resulted in about equal installed drag for both the rounded- and sharp-corner boattails.

2. Good agreement existed between flight and 1/20-scale wind tunnel results for the installed boattail drag of a VFE nozzle with a sharp-corner boattail except near Mach 1.0.

3. The sharp-corner VFE-type nozzle benefited the most from the airframe installation effects since its performance was improved across the entire speed range.

4. Installation of a plug nozzle had little effect on performance below Mach 0.89. Near Mach 0.95 a significant improvement was measured as the terminal shock was located near the nozzle, and above Mach 0.97 a large adverse effect occurred after the terminal shock moved off the nozzle.

5. For an installed AIE nozzle, decreased boattail drag in the high subsonic speed region was apparently offset by poor auxiliary inlet performance, making the installed and isolated performance about equal.

6. These installation effects were caused by the combination of the recompression in the flow fields of the wing and nacelle in the region of the exhaust nozzles. This was particularly effective in increasing pressures on a sharp-corner boattail.

7. The effect of increasing angle-of-attack on boattail drag was generally small for angles less than 8.5°.

8. In 1/20-scale model investigations, large variations in nacelle shape had little effect on boattail drag for conventional nacelle configurations.

SYMBOLS

A_n	nacelle cylindrical cross-sectional area
A_p	nozzle primary throat area
b	wing span
C_{D_β}	boattail pressure drag coefficient based on cross-sectional area at boattail juncture
C_p	static pressure coefficient
D	sum of nozzle external pressure and skin fraction drags
d	nacelle diameter
F	nozzle gross thrust
F_{ip}	ideal thrust of nozzle primary flow
M_0	free-stream or flight Mach number
R	nozzle boattail juncture radius
x	axial distance
y	spanwise distance
α	angle-of-attack

REFERENCES

1. Nichols, Mark R.: Aerodynamics of Airframe-Engine Integration of Supersonic Aircraft. NASA TN D-3390, 1966.

2. Mikkelson, Daniel C.; and Head, Verlon L.: Flight Investigation of Airframe Installation Effects on a Variable Flap Ejector Nozzle of an Underwing Engine Nacelle at Mach Numbers from 0.5 to 1.3. NASA TM X-2010, 1970.

3. Crabs, Clifford C.; Mikkelson, Daniel C.; and Boyer, Earle O.: An Inflight Investigation of Airframe Effects on Propulsion System Performance at Transonic Speeds. Presented at the 13th Annual Symposium of the Society of Experimental Test Pilots, Los Angeles, Calif., Sept. 25-27, 1969.

4. Blaha, Bernard J.; and Mikkelson, Daniel C.: Wind Tunnel Investigation of Airframe Installation Effects on Underwing Engine Nacelles at Mach Numbers from 0.56 to 1.46. NASA TM X-1683, 1968.

5. Blaha, Bernard J.; Mikkelson, Daniel C.; and Harrington, Douglas E.: Wind Tunnel Investigation of Installation Effects on Underwing Supersonic Cruise Exhaust Nozzles at Transonic Speeds. NASA TM X-52604, 1969.

6. Blaha, Bernard J.: Effect of Underwing Engine Nacelle Shape and Location on Boattail Drag and Wing Pressures at Mach Numbers from 0.56 to 1.46. NASA TM X-1979, 1970.

7. Harrington, Douglas E.: Jet Effects on Boattail Pressure Drag of Isolated Ejector Nozzles at Mach Numbers from 0.60 to 1.47. NASA TM X-1785, 1969.

8. Samanich, Nick E.; and Burley, Richard R.: Flight Performance of Auxiliary Inlet Ejector and Plug Nozzle at Transonic Speeds. Presented at the Sixth Propulsion Joint Specialist Conference, San Diago, California, June 15-19, 1970.

9. Harrington, Douglas E.: Effect of a Rectangular Simulated Wing on the Pressure-Drag Coefficient of Various Boattails at Mach Numbers from 0.60 to 1.47. NASA TM X-52609, 1969.

10. Martlew, D. L.: Noise Associated with Shock Waves in Supersonic Jets. Aircraft Engine Noise and Sonic Boom. AGARD-CP-42, May 1969.

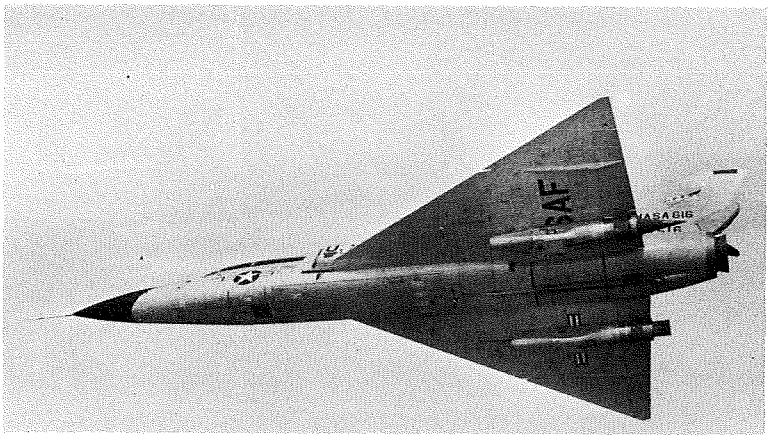

C-69-2871

Figure 1. - F-106 research flight with plug nozzle.

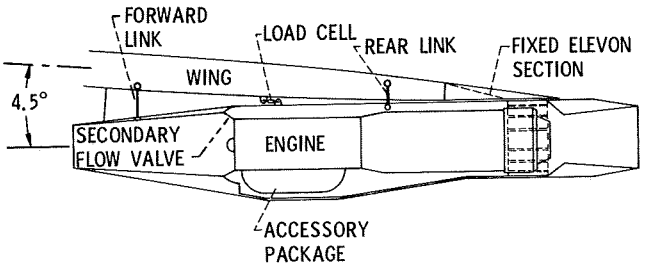

Figure 2. - Nacelle-engine installation.

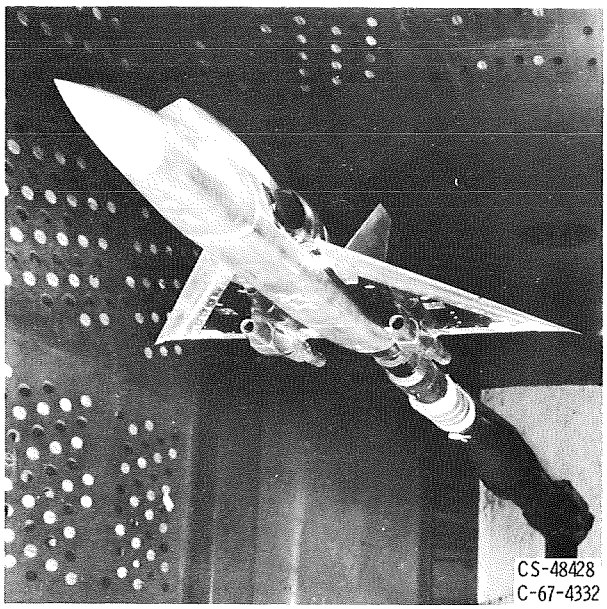

Figure 3. - 1/20th scale model of F-106 in 8- by 6-Foot Supersonic Wind Tunnel.

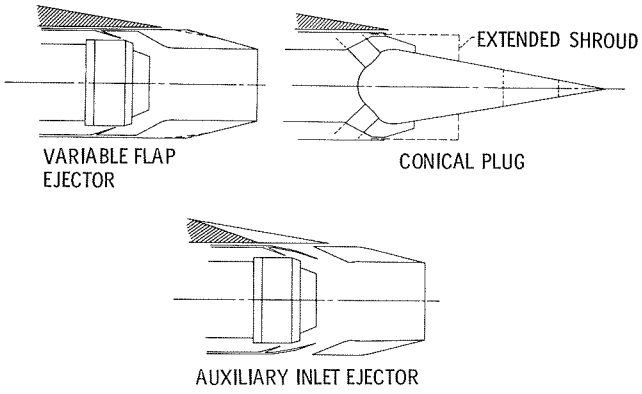

Figure 4. - Nozzles for F106 program.

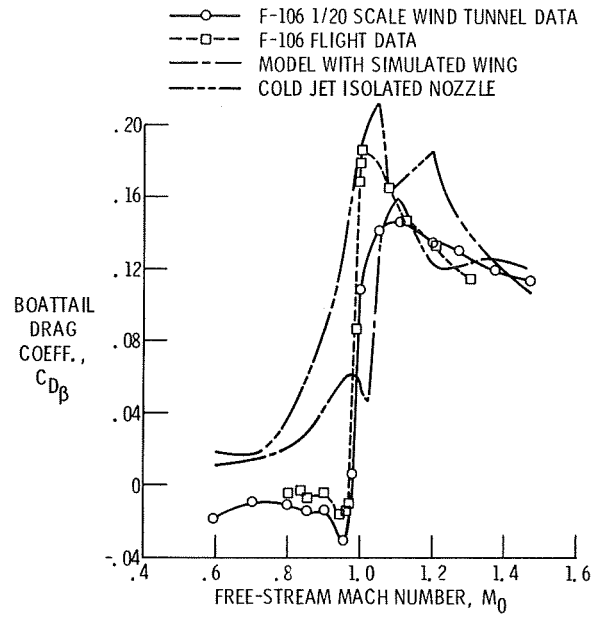

Figure 5. - Comparison of flight and wind tunnel data. 15° Conical boattail. R/d = 0, α = 2.5°.

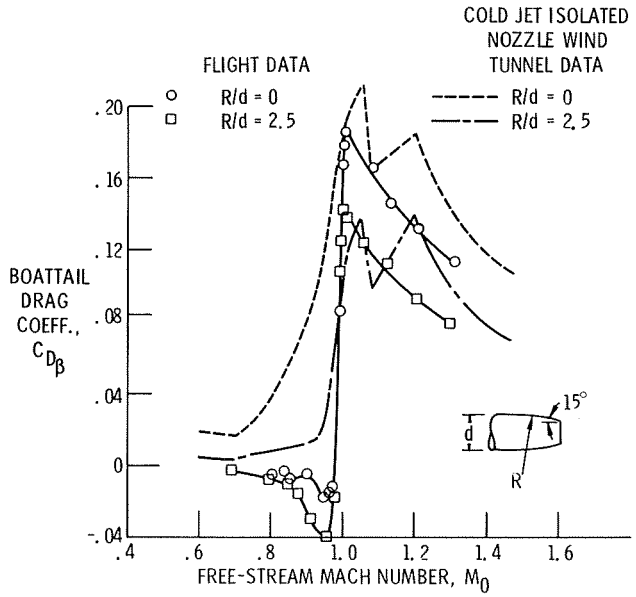

Figure 6. - Effect of afterbody shape on boattail drag. α = 0°.

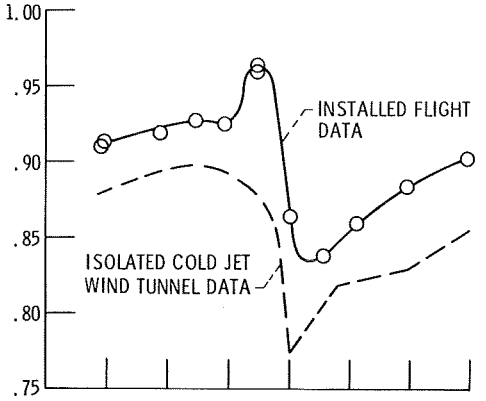

(a) Variable flap ejector nozzle. $A_p/A_n = 0.26$, R/d = 0.

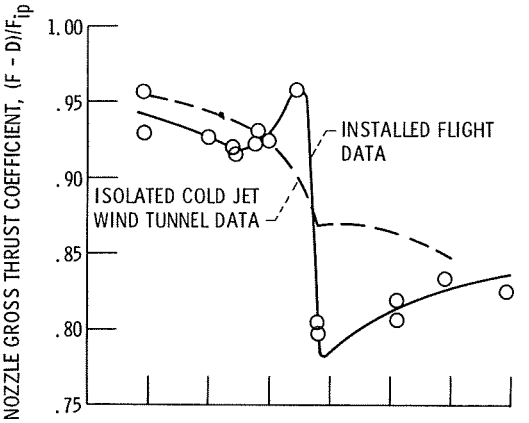

(b) Conical plug nozzle. $A_p/A_n = 0.22$.

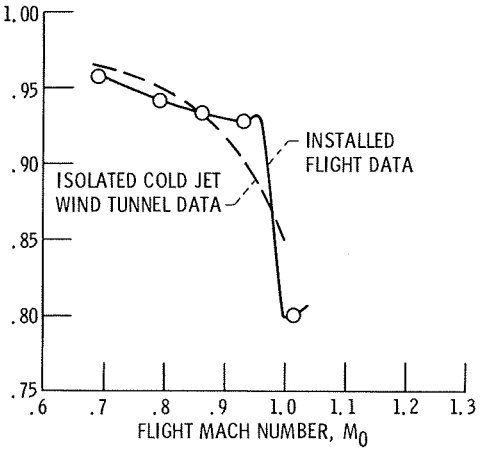

(c) Auxiliary inlet ejector nozzle. $A_p/A_n = 0.26$, R/d = 0.5.

Figure 7. - Installation effect on nozzle performance.

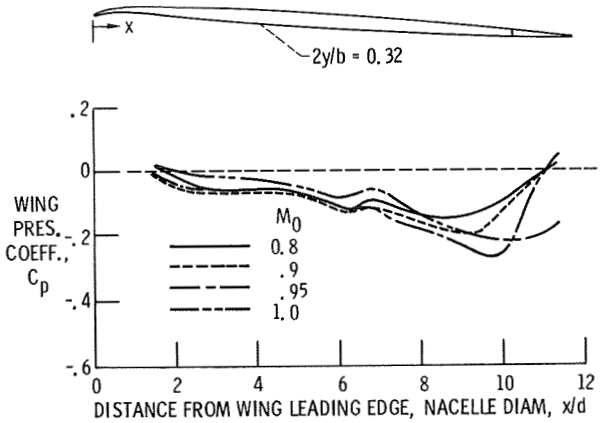

Figure 8. - Average wing lower surface pressure distribution without nacelle; 2y/b from 0.20 to 0.43. $\alpha = 2.5°$.

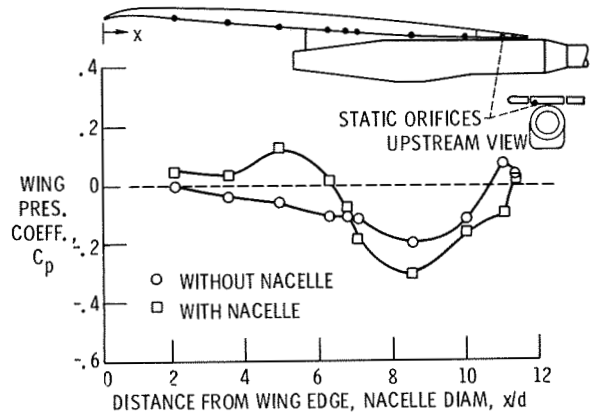

Figure 9. - Installation effect on wing pressure distribution. $M_0 = 0.85$; $\alpha = 2.5°$.

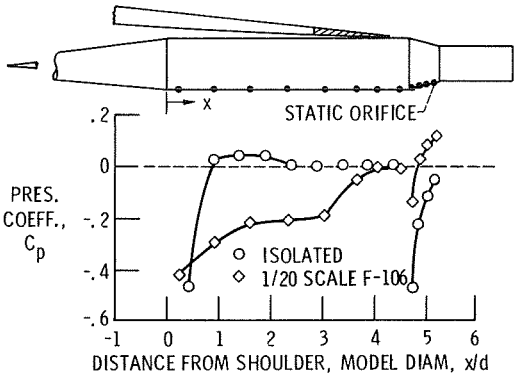

Figure 10. - Installation effect on nacelle pressures. $M_0 = 0.95$, $R/d = 0$, $\alpha = 0°$.

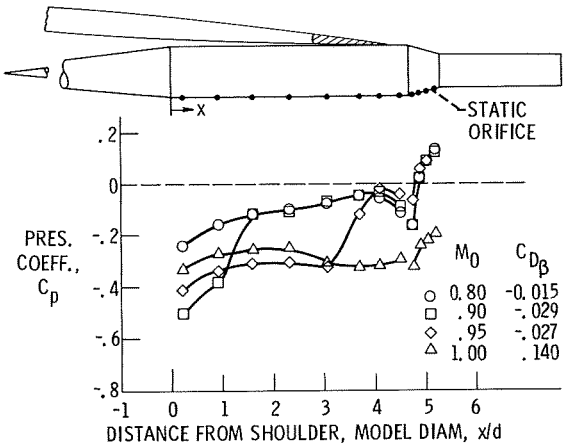

Figure 11. - Effect of Mach number on nacelle pressures. $R/d = 0$, $\alpha = 0°$.

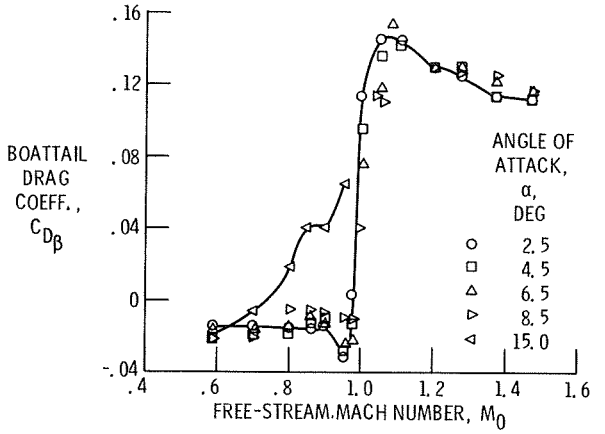

Figure 12. - Effect of angle of attack on boattail drag. R/d = 0.

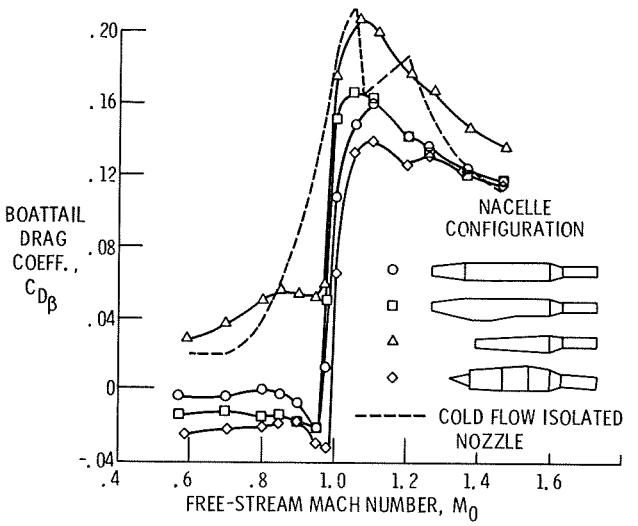

Figure 13. - Effect of nacelle shape on boattail drag. R/d = 0, α = 2.5°.